Laterally Ordered Bulk Heterojunction of Conjugated Polymers: Nanoskiving a Jelly Roll**

By *Darren J. Lipomi, Ryan C. Chiechi, William F. Reus,* and *George M. Whitesides**

This paper describes the fabrication of a nanostructured heterojunction of two conjugated polymers by a three-step process: i) spin-coating a multilayered film of the two polymers, ii) rolling the film into a cylinder (a ''jelly roll'') and iii) sectioning the film perpendicular to the axis of the roll with an ultramicrotome (nanoskiving). The conjugated polymers are poly(benzimidazoben-zophenanthroline ladder) (BBL, n-type) and poly(2-methoxy-5-(2′-ethylhexyloxy)-1,4-phenylenevinylene) (MEH-PPV, p-type). The procedure produces sections with an interdigitated junction of the two polymers. The spacing between the phases is determined by spin-coating (~15 nm to 100 nm) and the thickness of each section is determined by the ultramicrotome (100 to 1000 nm). The minimum width of the MEH-PPV layers accessible with this technique (~15 nm) is close to reported exciton diffusion lengths for the polymer. When placed in a junction between two electrodes with asymmetric work functions (tin-doped indium oxide (ITO) coated with poly(3,4-ethylenedioxythiophene:poly(styrenesulfonate) (PEDOT:PSS), and eutectic gallium-indium, EGaIn) the heterostructures exhibit a photovoltaic response under white light, although the efficiency of conversion of optical to electrical energy is low. Selective excitation of BBL with red light confirms that the photovoltaic effect is the result of photoinduced charge transfer between BBL and MEH-PPV.

1. Introduction

This paper describes the fabrication of a heterojunction of two conjugated polymers in which laterally thin (~15 to 100 nm) but vertically tall (100 to 1000 nm) phases are intimately packed and oriented perpendicularly to a substrate. The process used in the fabrication has three steps: i) spin-coating a composite film with 100 alternating layers of poly(benzimidazobenzophenanthroline ladder) (BBL, ''n-type'') and poly(2-methoxy-5-(2′-ethylhexyloxy)-1,4-phenylenevinylene) (MEH-PPV, ''p-type''); ii) rolling this multilayer film into a cylinder (a ''jelly roll''); and iii) sectioning the jelly roll with an ultramicrotome (nanoskiving,[1–6] Fig. 1). The cross-section of a slab of the jelly roll has an interdigitated arrangement of the two polymers. The thickness of the slab is determined by the ultramicrotome and the spacing between the two materials is determined by spin-coating.

Heterojunctions with designed order have been proposed for organic photovoltaic (OPV) devices, for which nano-structuring of the n-type and p-type phases with a spacing close to the exciton diffusion length (5 to 20 nm) within the photoactive layer would facilitate efficient separation of charges.[7] The structure described here provides an example of a rationally ordered heterojunction composed entirely of conjugated polymers and arranged on the length scale that characterizes exciton diffusion. We suggest that this approach to such structures could be useful in photophysical studies, and might ultimately suggest new approaches to OPV devices.

1.1. Background

1.1.1. Conjugated Polymer Heterostructures

The tunable optical and electronic properties, mechanical flexibility, and relatively low cost of conjugated polymers have motivated research into their use as the active components of many devices traditionally associated with inorganic semiconductors: particular interest has focused on polymer light-emitting devices,[8,9] field-effect transistors,[10] nanowires,[11] and photovoltaic devices.[12] Conjugated polymers, however, are often fundamentally incompatible with traditional methods for nanofabrication developed for inorganic semiconductors. Several creative techniques now exist for the fabrication of single-component structures.[13,14] This work is focused on developing routes to structures comprising multiple components.
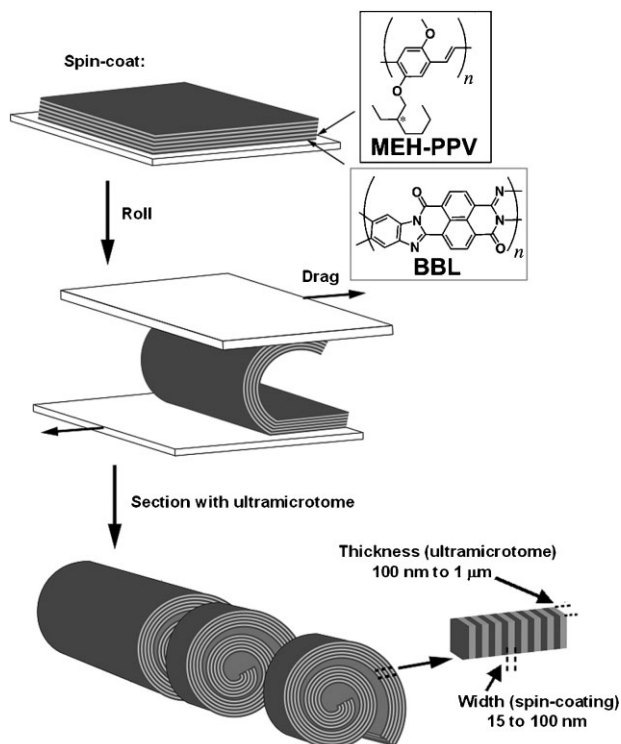
Figure 1. Brief summary of the procedure used to fabricate nanostructured heterojunctions from sectioning a jelly roll made of conjugated polymers. Spin-coating in an alternating fashion yields a composite film of the conjugated polymers, BBL (n-type) and MEH-PPV (p-type). Rolling this composite film into a jelly roll increases the density of material in the cross-section. An ultramicrotome sections the jelly roll into thin slabs. The cross-section of an individual slice has a structure with an interdigitated arrangement of the two polymers. The ultramicrotome determines the thickness of each slab, while spin-coating determines the width of each material within the heterojunction.

1.1.2. Mechanism of OPV Devices

When a photon is absorbed in an organic semiconductor, the low dielectric constant of the medium impedes the dissociation of the resulting electron-hole pair (called an exciton). The exciton can diffuse a characteristic length – the exciton diffusion length (L_D) – before it either decays, or reaches a boundary with another material. Devices that work by this so-called excitonic mechanism[15] require an interface between an electron donor ("p-type") and an electron acceptor ("n-type")[16] with offset frontier molecular orbitals (HOMO–LUMO energy levels) to enable the generation of free charge carriers. An excited electron in the LUMO of the p-type material transfers to the lower LUMO of the n-type material. Conversely, a hole created in the HOMO of the n-type material transfers to the higher HOMO of the p-type material. These changes in free energy provide the driving forces for the dissociation of excitons into free charge carriers. Once dissociated from each other, the electrons migrate by hopping among the LUMO(s) of the n-type material toward a low-work-function electrode (LWFE) and the holes migrate through the HOMO(s) of the p-type material toward a high-work-function electrode (HWFE). Ideally, all regions in the

active layer should be situated less than one L_D (typically 5 to 20 nm) from an interface between phases.

A competing criterion for efficient harvesting of photons, however, requires that the active layer have sufficient thickness to absorb the majority of incident photons (typically 100 to 200 nm).[17] Most organic heterojunctions are of two general configurations: the planar heterojunction and the bulk heterojunction. Planar heterojunctions consist of stacked thin films in the structure of HWFE/p-type/n-type/LWFE, where "p-type/n-type" denotes a 2D interface within the photoactive layer. In the planar configuration, only excitons created near the interface can contribute to the photovoltaic effect.[7] The bulk heterojunction has the form HWFE/p-type:n-type/LWFE, where "p-type:n-type" indicates a disordered, co-deposited layer of materials. The photoactive layer is usually a conjugated polymer (p-type) combined with a fullerene derivative (n-type). Co-deposition of the active layer increases the amount of interfacial area within the photoactive layer, but also destroys the complete continuity of each phase and provides little control over which material is in contact with which electrode. Despite these shortcomings, and the fact that the efficiencies of these devices are extremely sensitive to processing conditions,[7,18,19] bulk heterojunctions can exhibit quantitative photoluminescence quenching[20] and can be fairly efficient when incorporated into OPV devices ($\sim$5%).[21,22]

1.1.3. The Ordered Bulk Heterojunction

Recent reviews[7,17] and theoretical studies[23,24] have suggested that the ideal heterojunction would have a nanostructured network of the n-type and p-type materials preserving the physical continuity of each material both within the photoactive layer and to the proper electrodes. Structures that meet these criteria are called "ordered bulk heterojunctions"[17] (Fig. 2). The length scale of the nanostructuring should be close to L_D, in order to maximize the probability that an exciton formed in one material would reach the interface with the complementary material before de-excitation. A few organic-inorganic hybrid devices have been described in which
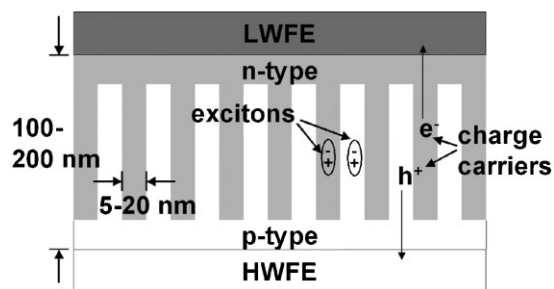
Figure 2. Schematic drawing of the cross-section of an ordered bulk heterojunction proposed for OPV devices. The architecture has a cross-section with an interdigitated arrangement of n-type and p-type phases. The width of each phase should be close to the exciton diffusion length (5 to 20 nm), while the thickness of the device should allow efficient collection of photons (100 to 200 nm for many conjugated polymers). This arrangement maximizes the probability than an exciton will reach an interface, where it can dissociate into two charge carriers, a hole (h^+) and an electron (e^-).

a conjugated polymer combines with an inorganic electron acceptor in an ordered fashion on the nanometric scale. For example, Alivisatos and co-workers cast poly(3-hexylthiophene) over vertically oriented CdTe nanocrystals,[25] and McGehee and co-workers infiltrated this polymer into nanoporous TiO_2.[26] These processes give photoactive layers with well-defined networks and straight, uninterrupted pathways to the electrodes. All-organic devices, in contrast, have not achieved the level of control attainable with organic-inorganic systems, although the use of block copolymers,[27] polymer demixing,[28] nanoimprinting,[29] controlled organic vapor-phase deposition[30] and photoinduced mass transport using an all-optical technique[31] have yielded interesting new heterostructures that satisfy some of the criteria required for an ordered bulk heterojunction.

1.2. Experimental Design

1.2.1. Nanoskiving

"Nanoskiving" is the name we have given to the use of an ultramicrotome for creating functional nanostructures by sectioning thin films;[1–6,32] it is a form of edge lithography.[33] We have applied nanoskiving to the fabrication of an ordered bulk heterojunction by spin-coating a composite film of alternating layers of p-type and n-type polymers on a planar substrate (in which the thickness of each layer is $L_D \sim 5$ to 20 nm), rolling the film to increase the density of the alternating layers within the structure, and obtaining sections of the thickness at which light absorption is optimal (100 to 200 nm).[7] This procedure would allows us, in principle, to "dial in" the spacing between the two materials (using spin-coating) and the thickness of the heterojunction (using nanoskiving).

1.2.2. Selection of Conjugated Polymers

The first step in the procedure was the generation of a free-standing, composite film of n-type and p-type materials. In choosing the two polymers, it was essential that we could deposit one on top of the other in a process that left the properties of both intact. The work of Jenekhe and coworkers established poly(benzimidazobenzophenanthroline ladder) (BBL) and poly(2-methoxy-5-(2′-ethylhexyloxy)-1,4-phenylene vinylene) (MEH-PPV) as one of the most effective n-type/p-type pairs that can be processed from orthogonal solvents to make a planar OPV device.[34] BBL is an n-type conjugated ladder polymer that has an ionization energy (HOMO level) of 5.9 eV, an electron affinity (LUMO level) of 4.0 eV, excellent thermal stability in air (≥500 °C),[35] and exceptionally high field-effect electron mobility.[36] MEH-PPV is a highly fluorescent p-type polymer with HOMO level of 5.1 eV and a LUMO level of 2.9 eV.[34] The exciton diffusion length of MEH-PPV has been measured using a variety of techniques in the literature,[37] but typically falls between 5 and 14 nm.[38,39] BBL and MEH-PPV are processed from methanesulfonic acid

and chloroform, respectively. These materials could be iteratively spin-coated on top of each other, because chloroform neither swells nor dissolves BBL and methanesulfonic acid neither swells nor dissolves MEH-PPV.

1.2.3. Selection of Electrodes

We used two electrodes with different work functions. Tin-doped indium oxide (ITO, work function = 4.7–4.8[40]), spin-coated with a thin film of the hole-selective polymer blend, poly(3,4-ethylenedioxythiophene):poly(styrenesulfonate) (PEDOT:PSS) was the HWFE. This electrode is highly transmissive in the visible region. PEDOT:PSS smoothes the surface of ITO and facilitates the injection of holes into the jelly roll, but does not itself produce a photovoltaic response.[41] We also required an electrode with a work function lower than that of ITO, in order to break the symmetry of the jelly roll and bias the photogenerated charge carriers to drift toward the proper electrodes.[42] For the LWFE we used the liquid eutectic gallium indium (EGaIn); this material substitutes for evaporated Al, which is commonly used.[43] EGaIn is conformal, convenient, and does not require the potentially damaging step of physical vapor deposition.[44] Figure 3A shows the positions of the work functions (for ITO, PEDOT:PSS and EGaIn) and the HOMOs and LUMOs (for BBL and MEH-PPV). Figure 3B shows a schematic illustration

Figure 3. A) Energy level diagram showing the vacuum-level positions of work functions (for ITO, PEDOT:PSS and EGaIn) and HOMOs and LUMOs (for BBL and MEH-PPV). B) Schematic illustration of the junction used 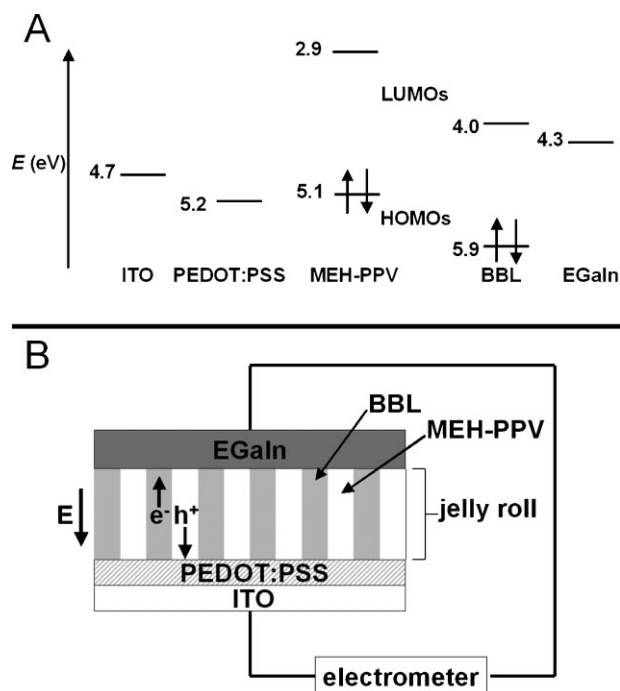to measure a photovoltaic response of a jelly roll. Under short-circuit conditions, a weak electric field E develops across the junction that biases the drift of photogenerated electrons (e⁻) and holes (h⁺) toward the EGaIn and the ITO.

of the experimental setup and the direction of charge carriers in the junction. The asymmetry of the electrodes creates a weak electric field, **E**, which, in principle, causes electrons (e^-) and holes (h^+) to drift toward the proper electrodes.

2. Fabrication

We fabricated two jelly rolls with different characteristics (Fig. 4). We made the first by spin-coating relatively thick layers (100 nm) of the conjugated polymers: sectioning this structure would allow proof of principle, and be easy to image. The second jelly roll tested how thin we could spin-coat layers of the conjugated polymers. We formed 50 layers of BBL
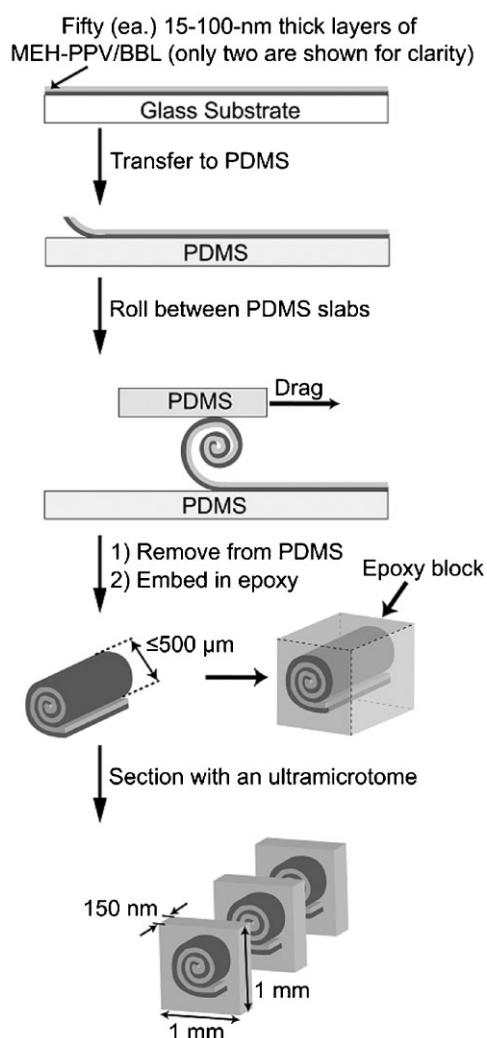
($\leq$100 nm), alternating with 50 layers of MEH-PPV ($\leq$100 nm), onto glass, by successive cycles of spin-coating. The substrate was immersed in deionized water after each layer of BBL (to remove methanesulfonic acid) and dried with a stream of N_2. After annealing the substrate at 125 °C under vacuum, sonication in methanol partially separated the layered film from the glass. We used tweezers to place a rectangular ($\sim$5 × 10 mm) piece of the film on a flat piece of poly (dimethylsiloxane) (PDMS), and dragged a second piece of flat PDMS over the top of the film. The film rolled into a jelly roll ($\sim$5 to 10 mm long and $\sim$500 µm in diameter). We embedded the jelly roll in epoxy and sectioned it with an ultramicrotome equipped with a diamond knife into square slices ($h = 150$ nm, l, $w \sim 1$ mm).[3]

3. Results and Discussion

3.1. Imaging

The first ("thick") jelly roll yielded a spiral structure when embedded in epoxy and sectioned with the ultramicrotome (see optical image, Fig. 5A). Figure 5B is a scanning electron
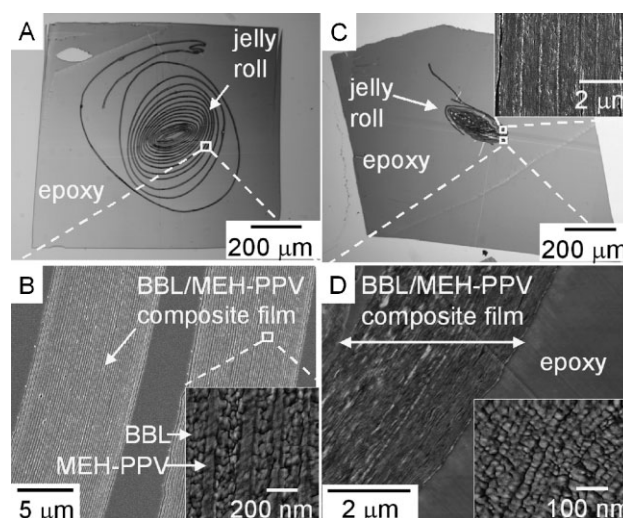

Figure 4. Summary of the procedure used to fabricate the polymer jelly roll. We spin-coated a free-standing film incorporating 50 layers of BBL alternating with 50 layers of MEH-PPV onto glass. We peeled the composite film from the substrate, and transferred it to a slab of poly(dimethylsiloxane) (PDMS). We dragged a second piece of PDMS over the top of the film. This action rolled the film into a loose cylinder, which we subsequently embedded in epoxy. Sectioning of the film with the ultramicrotome yielded individual slices ($l = 1$ mm, $w = 1$ mm, $h = 150$ nm).

Figure 5. Images of the polymer jelly rolls. A) Optical (bright-field) image of a 150-nm-thick slice of the "thick" jelly roll embedded in an epoxy membrane. B) Scanning electron micrograph (SEM) close-up of a region like the one indicated by the white box in (A). The exposed, 1-µm-thick, 100-layer film contains clearly defined, alternating layers of BBL and MEH-PPV. The average thickness of each phase is 100 nm. The inset is an atomic force micrograph (AFM tapping mode, phase image, range = 30°) of a region of the exposed composite film, which exhibits sharp boundaries between the layers. C) Optical image of the "thin" jelly roll. The composite film from which this structure was rolled was 2.5 µm thick and was composed of 50 layers of BBL ($\sim$35 nm) alternating with 50 layers of MEH-PPV ($\sim$15 nm). The inset is a SEM close-up region of three 2.5-µm strands, closely packed (the region shown has $\sim$300 parallel structures across). D) AFM height image of a region of the exposed BBL/MEH-PPV composite film shown in (B) (range = 52.5 nm). The inset is an AFM phase image of the exposed composite film (range = 30°). We measured a surface roughness (rms) of 6 nm for the exposed film and 0.5 nm for the surrounding epoxy. The inset is a close-up phase image of the exposed composite film.

micrograph (SEM) that shows two strands of the exposed surface of the BBL/MEH-PPV film. The exposed cross section of the film comprises 50 100-nm-thick layers of BBL and 50 of MEH-PPV. The structure is essentially a bicontinuous heterostructure of parallel nanowires. The inset is an atomic force micrograph (AFM, phase) of a region of the exposed polymer film and shows the clean separation between the BBL and the MEH-PPV phases.

The second (''thin'') jelly roll rolled into a tighter structure than the ''thick'' jelly roll (Fig. 5C). For the ''thin'' jelly roll, the average thickness of each layer was 25 nm. We estimated from the SEM that the BBL layers were closer to ~35 nm and the MEH-PPV layers were ~15 nm, although the accumulation of imperfections in the composite film led to non-uniform spacing of the two polymers. Independent measurement by profilometry of these films spin-coated under the same conditions on a Si/SiO$_2$ wafer gave heights of 40 nm and 20 nm for BBL and MEH-PPV. We estimate that the roughly elliptical area defined by the jelly roll in 5C contains ≤10% embedding epoxy.

The surface profile of the active material in the section would influence the ability to contact the top and bottom of the structure with electrodes. We obtained AFM profiles of the ''thin'' jelly roll (see Fig. 5D and the inset phase image): the rms roughness of the BBL/MEH-PPV film was 6 nm; that of the epoxy matrix was 0.5 nm.

We examined the cross section of the ''thin'' jelly roll by cutting a perpendicular cross section of a 1-μm-thick slice of the original structure. Figure 6 shows the interdigitated arrangement of the BBL/MEH-PPV composite film (compare Fig. 6 to Fig. 2). The image also qualitatively verifies the roughness (as seen by AFM) of the top and bottom of the composite film. Sectioning with the diamond knife does not appear to smear the surfaces of the polymer films.

3.2. Evidence of Photoinduced Charge Transfer within Jelly Roll by Measurement of Photovoltaic Response

We screened the heterostructures for a photovoltaic responses by placing sections of the ''thin'' jelly roll between a transparent electrode composed of an ITO-coated glass slide with a thin transparent film of PEDOT:PSS (20 nm) and a drop
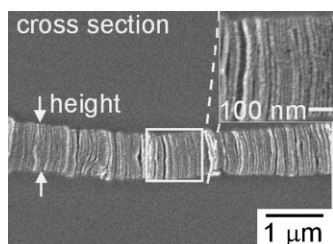
Figure 6. SEM of a cross-section of a 1-μm-thick section of the jelly roll derived from the 2.5-μm film (shown in Figure 5C and D). This image shows the orientation that the BBL/MEH-PPV layers would have in an OPV device. The inset is a close-up, which shows the dense packing of BBL (lighter shades) and MEH-PPV (darker shades) within the cross-section.
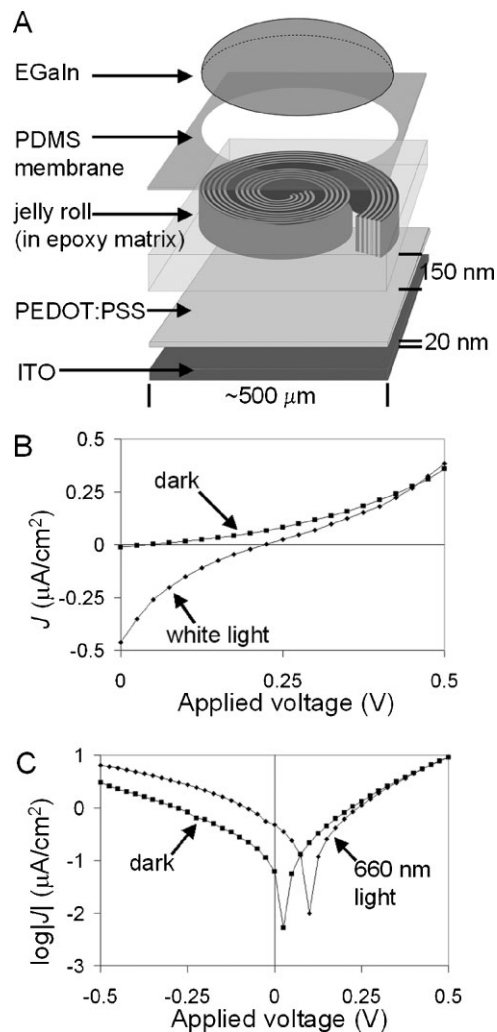
Figure 7. A) Schematic drawing of the electronic setup to measure the photovoltaic response of a jelly roll. We illuminated the junction from the bottom. B) Representative current versus voltage (J–V) data of the PV response from a 150-nm-thick section of the ''thin'' jelly roll in the dark (squares) and under white light illumination from a halogen source (diamonds). C) A plot of log|J| versus V for a different junction in the dark and illuminated by a red LED with λ_{max} = 660 nm.

of EGaIn (Fig. 7A). We used a poly(dimethylsiloxane) (PDMS) membrane containing a circular hole to prevent EGaIn from spilling over the jelly roll (shorting the device).[45–47]

We illuminated jelly rolls using white light (halogen source, flux ~100 mW cm^{-2}).[48] Figure 7B shows a representative plot of the current density (J) versus voltage (V). We determined the open-circuit voltage (V_{oc}, V) of the device by measuring the applied voltage required to bring the current to zero. The short-circuit current density (J_{sc}, mA cm^{-2}) is the current density that flows under zero applied voltage. We measured a V_{oc} of 225 mV and a J_{sc} of 0.45 μA cm^{-2}. We approximated the area of the jelly roll for the calculation of the current density by assuming its shape was elliptical and by measuring the semi-major axes with the SEM (area = 3.2 × 10^{-4} cm^2).[49] The area was not corrected for included epoxy, which made up ≤10% of the area of the

structure. The fill factor (*FF*) – the figure of merit that corresponds to the tendency of charge carriers to reach the electrodes rather than recombine – was 17%.

We tested >30 devices with this or similar configurations, and about half produced photovoltaic responses. The most common malfunctions were electrical shorting, probably through small cracks in the epoxy section or holes in a jelly roll through which the EGaIn made direct contact with the ITO/PEDOT:PSS electrode. The *J–V* curves typically overlapped upon repeated cycles (up to three) of applied voltage on a single junction. From junction to junction on a single substrate, the values of V_{oc} varied only slightly (± 50 mV) but the values of J_{sc} were reproducible within an order of magnitude.

3.2.1. Controls

We needed to demonstrate that i) the jelly roll itself produced the photovoltaic response (rather than PEDOT:PSS) and ii) photoinduced charge transfer within the jelly roll contributed to the photovoltaic response (rather than BBL or MEH-PPV acting independently). A control experiment with the junction ITO/PEDOT:PSS/EGaIn produced no photovoltaic response; this experiment demonstrated (i). Designing a control experiment for (ii) was necessary because MEH-PPV alone generates a V_{oc} in the configuration ITO/MEH-PPV/Al under white light illumination, whereas ITO/BBL/Al[34,40] and ITO/PEDOT:PSS/BBL/EGaIn do not. Illumination of a junction containing a jelly roll with a red light-emitting diode (LED) with $\lambda_{max} = 660$ nm (flux = 4.5 mW cm^{-2}), below the HOMO–LUMO gap of MEH-PPV, still produced a photovoltaic response. Illuminating a junction with the configuration ITO/PEDOT:PSS/MEH-PPV/EGaIn with the same LED did not produce a photovoltaic response. (As expected, white light did produce a weak photovoltaic response.) The only way, therefore, for the jelly roll to have produced a photovoltaic response under red light was for an exciton to be created in BBL, to reach an interface with MEH-PPV, and to transfer a hole to MEH-PPV. These observations, combined with the fact that BBL quenches $\geq 80\%$ of photoluminescence in MEH-PPV films ≤ 20-nm thick,[34] were consistent with the hypothesis that photoinduced charge transfer within the heterojunction contributed to or dominated the photovoltaic response of the jelly roll.

3.2.2. The Effect of Buffer Layers on Photovoltaic Performance

We investigated the use of "buffer layers" of MEH-PPV between the ITO and the jelly roll, and BBL between the jelly roll and the top electrode, as a first step toward improving the photovoltaic properties of these junctions. This experiment would ensure that the p-type and n-type phases made contact with only the HWFE and LWFE, respectively (compare Fig. 8A to the "ordered bulk heterojunction" of Fig. 2). We spin-coated a thin film of MEH-PPV (20 nm) on an ITO slide,
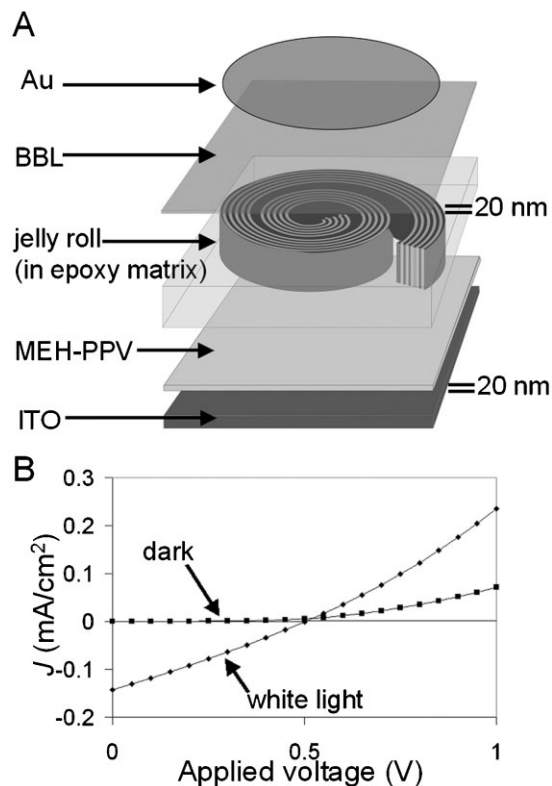

Figure 8. A) Schematic drawing of the electronic setup to measure the photovoltaic response of a jelly roll with buffer layers included between the jelly roll and the electrodes such that the BBL and the MEH-PPV made exclusive contact with the EGaIn and the ITO. B) A representative *J–V* plot shows that the devices produce a photovoltaic effect.

deposited a section of a jelly roll on the substrate, and spin-coated a layer of BBL on top of the jelly roll. Evaporation of an Au contact pad through a PDMS stencil finished the device.[50] See Figure 8A for a schematic drawing. A typical device displayed the following figures of merit (taken from Fig. 8B): $V_{oc} = 500$ mV, $J_{sc} = 0.15$ mA cm^{-2}, and $FF = 27\%$ (power conversion efficiency $\sim 0.02\%$). Note that J_{sc} is nearly 10^3 times higher than in the "no-buffer-layer" case. We attribute our relatively low values of J_{sc} to non-conformal contact of the jelly roll to the substrate. We tested >200 devices using buffer layers. The yield of devices that produced photovoltaic responses was over 60%. This configuration gave more reproducible *J–V* data from device to device than the "no-buffer-layer" configuration. When Au was used as the top contact, the values of V_{oc} varied between 500 and 550 mV, while the values of J_{sc} varied between 0.12 and 0.18 mA cm^{-2}.

4. Conclusions

This paper demonstrates nanoskiving as a technique for nanofabrication in thin-film polymer science, and suggests a potential application in organic photovoltaics. The technique converts the edge of a multilayered film into a densely packed

structure of macroscopic proportions (visible to the naked eye) that can be placed on almost any substrate for characterization. Further, it expands the capabilities of nanoskiving from metallic structures for optical applications to include organic components for electronic devices. The fabrication of the heterostructures is experimentally straightforward because it requires only a spin-coater and an ultramicrotome (instruments to which most researchers already have access). We were able to execute the entire process, from spin-coating to photovoltaic measurement, in about two days. We believe, therefore, that this technique will facilitate photovoltaic and photophysical investigation of n-type/p-type pairs of conjugated polymer structures arranged on the length scale of exciton diffusion.

This technique is not restricted to BBL and MEH-PPV – any "stackable" materials are suitable. They include other conjugated polymer pairs,[51,52] conjugated polyelectrolytes,[53] semiconductor nanocrystals,[47,54] physically deposited small molecules,[29] sol-gel precursors[55] and metal films alternating with metal oxides.[4] It should be possible, therefore, to form nanostructured heterojunctions of different compositions for different purposes. For example, this method would enable studies of photoluminescence quenching on pairs of materials that would not otherwise form an intimate heterojunction. We believe that the ultramicrotome is ideally suited to section thin-film electronic materials for the purposes of the characterization of materials or for the fabrication of test devices, and that nanoskiving could play an important role in the development of organic nanostructures.

5. Experimental

Fabrication of the "Thick" Jelly Roll (Fig. 5A and B and Photovoltaic Data in Fig. 7C): A glass slide was cut into a 2-cm square and spin-coated with BBL (obtained from Aldrich, made into a 0.5 wt% solution in methanesulfonic acid (MSA) (Fluka) prepared by dissolving 370 mg of polymer in 50 mL of MSA) at 3 krpm with a ramp rate of 1 krpm s^{-1} for 30 s. (MSA causes burns and should be spin-coated in a fume hood with the sash down. We generally used a homemade high-density polyethylene liner for the basin of the spin-coater, as MSA reacts slowly with aluminum foil.) The substrate was removed from the spinner with tweezers and immersed in deionized water for 5 s to remove MSA. The BBL film was dried with an N$_2$ gun, during which time the film changed from dark purple to light purple with a metallic gold luster. On top of the BBL film, we spin-coated MEH-PPV (purchased from Aldrich, avg. MW = 70,000–100,000, made into a 0.6 wt% solution in chloroform, prepared by dissolving 444 mg of polymer in 50 mL of chloroform) at 3 krpm with a ramp rate of 1 krpm s^{-1}. BBL and MEH-PPV films were stacked in this manner fifty times for 100 total layers of polymer with average thickness of 100 nm for each layer. The composite film was 10-μm-thick, as determined by SEM. The film was annealed under vacuum at 125 °C for 5 min, and scored around the edges of the glass substrate with a scalpel (in a square ∼1 mm from the edge of the glass). The substrate with the polymer film was immersed in methanol and placed in a sonicator bath for ∼20 s. This action delaminated the edges of the film from the glass. The film was then easily peeled off with tweezers, removed from the methanol and placed on a flat piece of poly(dimethylsiloxane) (PDMS) (Dow Coring Sylgard 184 kit, mixing cross-linker and prepolymer in a

ratio of 1:10). The multilayered film was cut into 1-cm squares with a razor blade. A 1-cm square of the PDMS was lubricated with a few drops of ethanol. A second piece of PDMS was dragged over the top of the film about 5 times in the same direction such that the film rolled into a cylinder. The "jelly roll" was embedded in epoxy prepolymer (Epo-Fix, obtained from Electron Microscopy Sciences, mixed and degassed before use), pressed with a wooden applicator to remove air bubbles, and cured at 60 °C for 2 h in a polyethylene mold (Electron Microscopy Sciences). The cooled block was cut with a hand saw to expose the cross section of the jelly roll. The block was trimmed and sectioned with the ultramicrotome (Leica Ultracut UCT, equipped with a diamond knife Diatome Ultra 35°) as described previously [3].

Fabrication of the "Thin" Jelly Roll (Figs. 5C, D, and 6; and Photovoltaic Data in Fig. 7B): This jelly roll was fabricated the same way as the first jelly roll, with the following modifications. 1) The first layer of BBL was spin-coated as before, successive layers were spin-coated from a 0.25 wt% solution at 3 krpm with a ramp rate of 1 krpm for 10 s (the BBL film directly touching the glass substrate had to be thick, otherwise it cracked during spinning). 2) MEH-PPV was spin-coated from a 0.12 wt% solution at 3 krpm with a ramp rate of 1 krpm for 10 s. The total thickness of the 100-layer film was 2.5 μm (as measured by SEM). The average thickness of each layer was 25 nm. Although individual layers were cast without major defects, the accumulation of minor imperfections in the composite film made the individual layers of BBL and MEH-PPV somewhat inhomogeneous, so it was difficult to measure accurate thicknesses of each layer. We estimate that the thickness of each BBL layer was approximately 35 nm and of each MEH-PPV layer was 15 nm. Profilometry (Veeco Dektak 6M Stylus Profilometer) of these films spin-coated under the same conditions on a Si/SiO$_2$ wafer gave heights of 40 nm and 20 nm for BBL and MEH-PPV.

Imaging: Optical images (Fig. 5A, C) were obtained using an optical microscope in bright field (Leica DMRX). Scanning electron microscope (SEM) images (Fig. 5B inset, Fig. 5C and inset, and Fig. 6) of the epoxy sections containing slices of the jelly roll were acquired with a LEO 982, Zeiss Ultra55, or Supra55 VP FESEM at 2 or 5 kV at a working distance of 2–6 mm. Before SEM imaging, some epoxy sections were placed on a silicon wafer and sputter coated with Pt/Pd at 60 mA for 15–45 s. Atomic force microscope (AFM) height (Fig. 5D) and phase (Fig. 5B inset, Fig. 5D inset) were obtained with a Veeco Dimension 3100 instrument using tapping mode.

Photovoltaic Measurements (Fig. 7): The "thin" jelly roll was used to obtain the photovoltaic data of Figure 7B. The "thick" jelly roll was used for Figure 7C. An ITO/SiO$_2$ slide (Delta Technologies, Ltd., 0.7 mm SiO$_2$, R_s = 4–8 Ω) was cut into a 2.5-cm square, washed with ethanol or acetone, and treated with oxygen plasma (1 min) prior to use. The slide was spin-coated with PEDOT:PSS (supplied by Aldrich as a 1.3 wt% dispersion in water, diluted by us 1:1 with deionized water) at 3 krpm with a ramp rate of 1 krpm s^{-1} for 60 s. The PEDOT:PSS was annealed at 125 °C in a vacuum oven for 15 min. The substrate was treated with oxygen plasma for 10 s in order to increase the wettability of the substrate. This action facilitates the transfer of epoxy sections from the water boat of the ultramicrotome to the substrate. Epoxy sections floating in the water bath of the diamond knife of the ultramicrotome were transferred with the Perfect Loop tool (Electron Microscopy Sciences) to the surface of the MEH-PPV-coated substrate. The substrate was placed in a vacuum desiccator until the water evaporated, leaving the epoxy sections adhered flatly to the substrate by way of capillary forces. Sections (5–10 per substrate) were then annealed in a vacuum oven at 125 °C for 15 to 60 min in order to remove wrinkles in the epoxy sections. We obtained a PDMS membrane patterned with circles (r = 0.5 mm) by a procedure described previously [45]. Pieces of the membrane were placed over the epoxy sections, such that the jelly rolls were exposed through the circular holes. Drops of EGaIn (Aldrich) were placed with a syringe on top of the exposed jelly rolls. The PDMS membrane prevented the EGaIn from spilling onto the substrate. Copper wires were placed in each drop of EGaIn and secured to the substrate with drops of

5-Minute Epoxy (Devcon). Devices were screened indoors for photovoltaic effect using a Keithley 6430 source meter and a halogen lamp with a flux of $100\,mW\,cm^{-2}$ as estimated (for Fig. 7B) using a Daystar Solar Meter and (for Fig. 7C) with a red LED with $\lambda_{max} = 660\,nm$ and flux $= 4.5\,mW\,cm^{-2}$ as determined using an optical power meter (ThorLabs DET 110). The ITO was the anode under positive bias, while the EGaIn was grounded.

Photovoltaic Measurements with "Buffer Layers" (Fig. 8): The second configuration differs from the first configuration in three ways. 1) Instead of PEDOT:PSS, MEH-PPV coated the ITO/SiO$_2$ substrate. The substrate was spin-coated with MEH-PPV (0.12 wt% solution in chloroform) at 3 krpm with a ramp rate of 1 krpm s^{-1} and treated with oxygen plasma for 1 s in order to assist transfer of the epoxy sections to the substrate. 2) After placement of the epoxy sections, the substrate was spin-coated with BBL (0.5 wt% in MSA, at a spin rate of 6 krpm with a ramp of 1 krpm s^{-1} for 30 s). The substrate was immersed in deionized water for at least 5 h, blown dry with a stream of N$_2$, and annealed under vacuum at 125 °C for 15 min. 3) After placing the PDMS membranes over the jelly rolls, the exposed regions of the substrate (except for the jelly rolls) were covered with sticky tape. The substrate was sputter-coated with Au ($\sim$100 nm). The PDMS membranes and the sticky tape were removed and placed fresh PDMS membranes over the jelly rolls, covered with a circular thin film of Au ($\sim$100 nm). The ends of several copper wires were dipped in graphite ink and placed in contact with the evaporated Au contacts. The graphite ink was allowed to dry overnight and the wires were secured to the substrate with drops of 5-minute epoxy. Photovoltaic measurements were carried out as in the first configuration.

[1] Q. Xu, R. M. Rioux, G. M. Whitesides, *ACS Nano* **2007**, *1*, 215.

[2] Q. B. Xu, J. M. Bao, F. Capasso, G. M. Whitesides, *Angew. Chem. Int. Ed.* **2006**, *45*, 3631.

[3] Q. B. Xu, J. M. Bao, R. M. Rioux, R. Perez-Castillejos, F. Capasso, G. M. Whitesides, *Nano Lett.* **2007**, *7*, 2800.

[4] Q. B. Xu, B. D. Gates, G. M. Whitesides, *J. Am. Chem. Soc.* **2004**, *126*, 1332.

[5] Q. B. Xu, R. Perez-Castillejos, Z. F. Li, G. M. Whitesides, *Nano Lett.* **2006**, *6*, 2163.

[6] D. J. Lipomi, R. C. Chiechi, M. D. Dickey, G. M. Whitesides, *Nano Lett.* **2008**, *8*, 4100–4105.

[7] S. Gunes, H. Neugebauer, N. S. Sariciftci, *Chem. Rev.* **2007**, *107*, 1324.

[8] J. H. Burroughes, D. D. C. Bradley, A. R. Brown, R. N. Marks, K. Mackay, R. H. Friend, P. L. Burns, A. B. Holmes, *Nature* **1990**, *347*, 539.

[9] I. D. W. Samuel, G. A. Turnbull, *Chem. Rev.* **2007**, *107*, 1272.

[10] H. Sirringhaus, P. J. Brown, R. H. Friend, M. M. Nielsen, K. Bechgaard, B. M. W. Langeveld-Voss, A. J. H. Spiering, R. A. J. Janssen, E. W. Meijer, P. Herwig, D. M. de Leeuw, *Nature* **1999**, *401*, 685.

[11] A. K. Wanekaya, W. Chen, N. V. Myung, A. Mulchandani, *Electroanalysis* **2006**, *18*, 533.

[12] B. C. Thompson, J. M. J. Fréchet, *Angew. Chem. Int. Ed.* **2008**, *47*, 58.

[13] S. Holdcroft, *Adv. Mater.* **2001**, *13*, 1753.

[14] E. Menard, M. A. Meitl, Y. G. Sun, J. U. Park, D. J. L. Shir, Y. S. Nam, S. Jeon, J. A. Rogers, *Chem. Rev.* **2007**, *107*, 1117.

[15] B. A. Gregg, *J. Phys. Chem. B* **2003**, *107*, 4688.

[16] We adopt the terms "p-type" or "n-type" to mean that the materials are principally used to transport holes or electrons, using typical electrode materials. For a discussion of the factors that influence charge transport in organic semiconductor, see: V. Coropceanu, J.

[17] Cornil, D. A. da Silva Filho, Y. Olivier, R. Silbey, J.-L. Brédas, *Chem. Rev.* **2007**, *107*, 926.

[17] K. M. Coakley, M. D. McGehee, *Chem. Mater.* **2004**, *16*, 4533.

[18] F. Padinger, R. S. Rittberger, N. S. Sariciftci, *Adv. Funct. Mater.* **2003**, *13*, 85.

[19] K. Sivula, C. K. Luscombe, B. C. Thompson, J. M. J. Fréchet, *J. Am. Chem. Soc.* **2006**, *128*, 13988.

[20] N. S. Sariciftci, L. Smilowitz, A. J. Heeger, F. Wudl, *Science* **1992**, *258*, 1474.

[21] W. L. Ma, C. Y. Yang, X. Gong, K. Lee, A. J. Heeger, *Adv. Funct. Mater.* **2005**, *15*, 1617.

[22] J. Peet, J. Y. Kim, N. E. Coates, W. L. Ma, D. Moses, A. J. Heeger, G. C. Bazan, *Nat. Mater.* **2007**, *6*, 497.

[23] B. Kannan, K. Castelino, A. Majumdar, *Nano Lett.* **2003**, *3*, 1729.

[24] L. G. Yang, L. Chen, R. Bai, F. Yang, M. Wang, H. Z. Chen, *Sol. Energy Mater. Sol. Cells* **2007**, *91*, 1110.

[25] I. Gur, N. A. Fromer, A. P. Alivisatos, *J. Phys. Chem. B* **2006**, *110*, 25543.

[26] C. Goh, K. M. Coakley, M. D. McGehee, *Nano Lett.* **2005**, *5*, 1545.

[27] U. Stalmach, B. de Boer, C. Videlot, P. F. van Hutten, G. Hadziioannou, *J. Am. Chem. Soc.* **2000**, *122*, 5464.

[28] F. A. Castro, H. Benmansour, C. F. O. Graeff, F. Nuesch, E. Tutis, R. Hany, *Chem. Mater.* **2006**, *18*, 5504.

[29] D. M. Nanditha, M. Dissanayake, A. Adikaari, R. J. Curry, R. A. Hatton, S. R. P. Silva, *Appl. Phys. Lett.* **2007**, *90*.

[30] F. Yang, M. Shtein, S. R. Forrest, *Nat. Mater.* **2005**, *4*, 37.

[31] C. Cocoyer, L. Rocha, L. Sicot, B. Geffroy, R. de Bettignies, C. Sentein, C. Fiorini-Debuisschert, P. Raimond, *Appl. Phys. Lett.* **2006**, *88*.

[32] Q. B. Xu, R. M. Rioux, M. D. Dickey, G. M. Whitesides, *Acc. Chem. Res.* in press.

[33] B. D. Gates, Q. B. Xu, M. Stewart, D. Ryan, C. G. Willson, G. M. Whitesides, *Chem. Rev.* **2005**, *105*, 1171.

[34] M. M. Alam, S. A. Jenekhe, *Chem. Mater.* **2004**, *16*, 4647.

[35] S. Y. Hong, M. Kertesz, Y. S. Lee, O. K. Kim, *Macromolecules* **1992**, *25*, 5424.

[36] A. Babel, S. A. Jenekhe, *J. Am. Chem. Soc.* **2003**, *125*, 13656.

[37] Scully and McGehee noted that exciton diffusion lengths are often overestimated due to effects of optical interference and energy transfer. They measured a diffusion length of (6 ± 1) nm for MDMO-PPV, a structural relative of MEH-PPV. See: S. R. Scully, M. D. McGehee, *J. Appl. Phys.* **2006**, *100*, 034907.

[38] A. J. Lewis, A. Ruseckas, O. P. M. Gaudin, G. R. Webster, P. L. Burn, I. D. W. Samuel, *Org. Electron.* **2006**, *7*, 452.

[39] D. E. Markov, C. Tanase, P. W. M. Blom, J. Wildeman, *Phys. Rev. B* **2005**, *72*.

[40] S. A. Jenekhe, S. J. Yi, *Appl. Phys. Lett.* **2000**, *77*, 2635.

[41] F. Zhang, O. Inganäs, in *Organic Photovoltaics: Mechanisms, Materials, and Devices* (Eds: S. S. Sun, N. S. Sariciftci), CRC Press, Boca Raton, FL **2005**, p. 479.

[42] The use of electrodes with asymmetric workfunctions is also necessary in bulk heterojunction devices, where the photoactive layer is a disordered network with both types of charge carriers distributed randomly throughout the device.

[43] A. Du Pasquier, S. Miller, M. Chhowalla, *Sol. Energy Mater. Sol. Cells* **2006**, *90*, 1828.

[44] M. D. Dickey, R. C. Chiechi, R. J. Larsen, E. A. Weiss, D. A. Weitz, G. M. Whitesides, *Adv. Funct. Mater.* **2008**, *18*, 1.

[45] R. J. Jackman, D. C. Duffy, O. Cherniavskaya, G. M. Whitesides, *Langmuir* **1999**, *15*, 2973.

[46] R. C. Chiechi, E. A. Weiss, M. D. Dickey, G. M. Whitesides, *Angew. Chem. Int. Ed.* **2008**, *47*, 142.

[47] E. A. Weiss, R. C. Chiechi, S. M. Geyer, V. J. Porter, D. C. Bell, M. G. Bawendi, G. M. Whitesides, *J. Am. Chem. Soc.* **2008**, *130*, 74.

[48] We estimated the flux of the halogen source with a commercial power meter calibrated for the solar spectrum.

[49] This method includes some of the epoxy membrane, which does not contribute to the photocurrent. Using only the area of the exposed BBL/MEH-PPV film would yield higher J_{sc} values (we estimate by $< 10\%$), but would not be as relevant from an engineering standpoint, where density of photoactive material within a section is critical.

[50] The asymmetry within the active layer imposed by the buffer layers allowed us to use Au as a top electrode, even though it has a higher work function than EGaIn. See ref. [15].

[51] M. Onoda, K. Tada, A. A. Zakhidov, K. Yoshino, *Thin Solid Films* **1998**, *331*, 76.

[52] S. R. Scully, P. B. Armstrong, C. Edder, J. M. J. Fréchet, M. D. McGehee, *Adv. Mater.* **2007**, *19*, 2961.

[53] A. Garcia, R. Yang, Y. Jin, B. Walker, T. Q. Nguyen, *Appl. Phys. Lett.* **2007**, *91*.

[54] I. Gur, N. A. Fromer, M. L. Geier, A. P. Alivisatos, *Science* **2005**, *310*, 462.

[55] J. Y. Kim, S. H. Kim, H. H. Lee, K. Lee, W. L. Ma, X. Gong, A. J. Heeger, *Adv. Mater.* **2006**, *18*, 572.